Quantum Electronics **31** (4) 293 – 297 (2001)

CONTROL OF LASER RADIATION PARAMETERS

PACS numbers: 42.55.Lt; 42.60.Jf
DOI: 10.1070/QE2001v031n04ABEH001937

Effect of inhomogeneities of an active medium on the divergence of radiation from a long-pulse electric-discharge XeCl laser

V F Losev, Yu N Panchenko

***Abstract*. The effect of optical inhomogeneities of the active medium of an electric-discharge XeCl laser excited by 300-ns pulses on the divergence of amplified radiation is experimentally studied. The possibility of obtaining the diffraction-limited divergence of radiation at the output of the amplifier is shown. Under our conditions, for the pump power density exceeding 400 kW cm^{-3}, the radiation divergence in mainly determined by the nonuniformity of the gain profile of the active medium that appears at a certain stage of the discharge burning. This property of the active medium is caused by the development of macro- and microinhomogeneities of the discharge current.**

Keywords: *excimer laser, active medium, wave-front distortions, divergence, inhomogeneity of a medium.*

1. Introduction

At present, electric-discharge excimer lasers find an increasing application in various fields of science and technology. Many applications require laser radiation with high energy and low divergence. The simultaneous obtaining of these two parameters is a serious challenge. This is explained by the fact that to increase the output energy of an excimer laser, one should increase its active volume or the duration of its pulse. As the active volume increases, the fraction of amplified spontaneous emission (ASE) in the output emission increases, while the increase in the pump pulse duration deteriorates the burning conditions of a homogeneous volume discharge. Therefore, in both cases, the factors appear that deteriorate the divergence of the output emission.

It is known that the fraction of ASE in the output laser emission can be decreased by using either unstable resonators [1] or the amplification regime [2]. The conditions of formation and burning of a homogeneous discharge in excimer mixtures with pulse durations of several hundreds of nanoseconds have been studied in papers [5 – 18]. It was shown that at a certain stage, inhomogeneities could emerge in the discharge at different spatial scales [9, 15, 16]. Macroinhomogeneities represent channels with an enhanced current density and a characteristic diameter of ~ 1 mm, while microinhomogeneities represent filamentary channels of diameter 0.01 – 0.1 mm. In addition, the discharge width can change during the pump pulse mainly due to the electric-field inhomogeneity [17, 18]. The inhomogeneities of the active medium not only decrease the laser output energy but also can quench lasing [6, 11, 15].

The degree of influence of the discharge inhomogeneity on the laser radiation divergence has been poorly studied so far. It was noted in papers [15, 16] that the laser pulse duration is mainly limited by scattering of radiation from optical microinhomogeneities of the active medium. The authors of paper [13] found that the divergence of radiation from a plane-parallel two-section XeCl laser emitting 300-ns pulses deteriorated after the operation of the first section of the active volume. The interferometric measurements of the parameters of the active medium of an electric-discharge XeCl laser pumped by 400-ns pulses [14] revealed small-scale variations in the refractive index, which were caused, in the opinion of the authors [14], by the gas-dynamic unloading of filamentary current channels appearing at the current pulse end.

In the presence of inhomogeneities in the active medium, the directivity of laser emission can be improved by using phase conjugation. It is known that phase conjugation allows one to correct phase distortions of the wave front caused by inhomogeneities of the medium [3, 4]. At present, no information is available in the literature on the possibility to use this method in long-pulse excimer lasers because phase conjugation has been mainly used in lasers with the lifetime of the active medium of the order of several tens of nanoseconds [19 – 22].

In this paper, we studied experimentally the effect of optical inhomogeneities of the active medium of an electric-discharge long-pulse XeCl laser on the angular directivity of its radiation and the possibility of correction for the wave-front distortions appearing in the active medium.

2. Experimental

We studied the active medium of an electric-discharge XeCl laser with the duration of a pulse of the first half-period of a discharge current equal to 300 ns. The discharge was ignited using a two-contour electric circuit containing the storage and peaking capacitors of capacity 110 and 10 nF, respectively. The storage capacitor was commuted via two spark gaps to the discharge gap, the peaking capacitor being connected in parallel.

V F Losev, Yu N Panchenko Institute of High-Current Electronics, Siberian Division, Russian Academy of Sciences, Akademicheskii prosp. 4, 634055 Tomsk, Russia

Received 26 December 2000
Kvantovaya Elektronika **31** (4) 293 – 227 (2001)
Translated by M N Sapozhnikov

Preionisation of the discharge gap was performed from a 'plasma sheet', which simultaneously served as a cathode, an anode being made of metal (Ni). The operating surface of both electrodes has a radius of 7 cm, the size of the active medium being 1.5 cm × 3.5 cm × 60 cm. The output windows of a laser chamber were made of quartz plates with antireflection coating. The output energy of the laser upon excitation of the Ne : Xe : HCl = 1400 : 10 : 1 mixture with a total pressure of 4 atm in the free-running mode with a plane-parallel resonator was 150 mJ.

The development of inhomogeneities in the active medium of the XeCl laser was detected by several methods. First, the time sweep of the discharge emission was detected with an Agat-SF3M streak camera. Second, we measured the distribution of the radiation intensity in the near-field zone of the probe beam that has passed through the active medium at different instants of time t (measurements were performed from the onset of the current pulse of the discharge to the probe pulse arrival). Because probing was preformed at 308 nm, the detected intensity distribution reflected the gain profile of the active medium. The effect of inhomogeneities on the angular directivity of the propagating radiation was determined from the distribution of its intensity in the far-field zone. Fig. 1 shows the optical schematic of experiments.

A short probe radiation pulse was formed in a laser system consisting of two lasers. One of them was used as a master oscillator (MO) and the other one, as an amplifier. A laser beam at the MO output has a diameter of 1.4 mm, an energy of 0.7 mJ, a FWHM pulse duration of 50 ns, a spectral width of 0.01 cm^{-1}, a polarisation degree of 95 %, and a nearly diffraction-limited divergence. The MO beam, after a preliminary 10-fold expansion with the help of a lens telescope, was amplified during one transit in the second laser. As a result, the probe radiation had a uniform intensity distribution over the beam cross section and an energy of 25 mJ. The probe pulse duration (FWHM) was 15 ns and its divergence was close to the diffraction-limited one for a diameter of 14 mm [23]. This radiation passed through an aperture of diameter 10 mm and propagated in the active medium of the long-pulse XeCl laser under study.

We corrected distortions of the wave front of the amplified radiation using phase conjugation upon SBS.

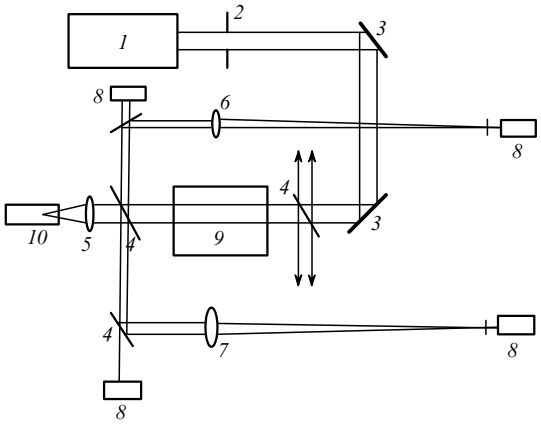

Figure 1. Optical schematic of the experiment: (*1*) laser system; (*2*) 10-mm aperture; (*3*) Al mirror; (*4*) quartz plate; (*5–7*) positive lenses with $F = 0.6$, 6, and 10 m, respectively; (*8*) detectors (FEK 22SPU, IMO-2N); (*9*) active medium of the XeCl laser; (*10*) cell with hexane.

The output radiation of the laser under study was focused by a lens with the focal length $F = 60$ cm to a cell of length 150 mm filled with hexane C_6H_{14}. Then, the scattered radiation was amplified during the back transit through the active medium. To achieve the high SBS efficiency and exclude thermal effects in the nonlinear medium, we chose the optimal input geometry and intensity of the probe beam [22–24].

The temporal profiles of the incident and scattered beams were measured with a FEK 22SPU photodiodes using 6LOR and S8-14 oscilloscopes. The radiation energy was detected with an IMO-2N power meter. The divergence of radiation was measured with a mirror wedge attenuator [25] and calibrated apertures in the focal plane of a lens with $F = 10$ m.

3. Experimental results and discussion

At the initial stage, after an electric breakdown in the long-pulse laser, a volume discharge was fed from the peaking capacitor. Because its discharge circuit had a minimum inductance, this capacitor provided a rapid energy input into the plasma. For this reason, the moment of generation of the radiation pulse with respect to the discharge current pulse remained virtually the same for all experimental conditions. However, the pulse duration and the ASE intensity substantially depended on the experimental conditions. The radiation pulse duration increased with decreasing charge voltage, pressure, and halogen concentration in the mixture (Fig. 2). A decrease in the xenon concentration from 30 to 7 Torr did not appreciably affect the ASE pulse duration under our conditions. The termination of the radiation pulse before the end of the first half-period of the current can be caused by the development of inhomogeneities in the discharge, although the shape and duration of current oscillograms only weakly depended on experimental conditions.

The amplification of the probe pulse in the active medium showed that the divergence of the output radiation could substantially depend on the pumping conditions. Fig. 3 shows the dependences of the fraction of energy of the amplified radiation at the central lobe of the radiation pattern on the charging voltage, pressure, and the halogen content in the mixture for the moment of the maximum pump power. One can see that the fraction of radiation energy for a pressure of 2 atm varies no more than by 40 % over the entire range of voltage and halogen concentration. For a pressure of 4 atm, a similar situation takes place only at low voltage and low halogen concentration. As the charging voltage and the HCl concentration increase, the radiation divergence substantially increases. These results well correlate with the data in Fig. 2 and show that the homogeneity of the volume discharge is improved with decreasing charging voltage, pressure, and the halogen concentration in the mixture.

We studied the effect of optical inhomogeneities on the radiation divergence under the conditions of a maximum gain obtained in the active medium for the specified pump pulse duration. This was achieved in our case in the Ne : Xe : HCl = 1400 : 10 : 1 mixture at the pressure $p = 4$ atm and the charging voltage $U_0 = 30$ kV. The profiles of the current and voltage at these conditions are shown in Fig. 4. The weak-signal gain at the maximum of the pump current is $g_0 = 0.05$ cm^{-1}. Note that this gain substantially varied

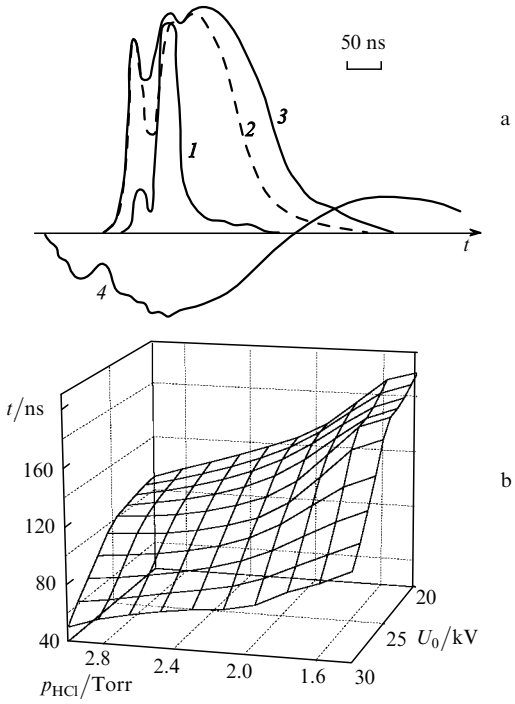

Figure 2. Oscillograms of ASE pulses (a) and the dependence of their FWHM duration on the HCl pressure and charging voltage at $p = 4$ atm and the ratio Ne : Xe = 100 : 1 (b); (*1*) the mixture pressure is $p = 4$ atm, the mixture composition is Ne : Xe : HCl = 1000 : 10 : 1, $U_0 = 30$ kV, the signal attenuation coefficient is $K = 20$; (*2*) $p = 4$ atm, Ne : Xe : HCl = 1800 : 10 : 1, $U_0 = 25$ kV, $K = 7$; (*3*) $p = 2$ atm, Ne : Xe : HCl = 1800 : 10 : 1, $U_0 = 20$ kV, $K = 1$; (*4*) the discharge current pulse shape at $p = 4$ atm, Ne : Xe : HCl = 1800 : 10 : 1, $U_0 = 25$ kV, and $K = 7$.

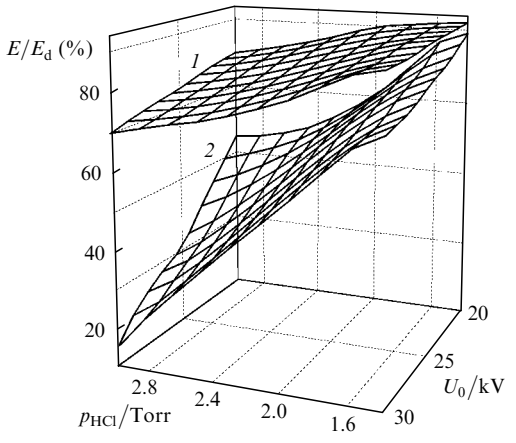

Figure 3. Fraction of the energy in the central lobe of the directivity diagram of the amplified short pulse at the instant of time $t = 100$ ns for Ne : Xe = 100 : 1 and the mixture pressure equal to 2 (*1*) and 4 atm (*2*).

over the volume and in time. Fig. 5 shows the densitograms of the discharge emission near the anode, which were obtained with an Agat streak camera. One can see that at $t = 120$ ns the discharge is abruptly contracted in the region of the maximum field strength.

Fig. 6 shows the intensity distributions of the probe beam propagated through the active medium at different instants of time. One can see from the radiation intensity distribution in the near-field zone that the width of the

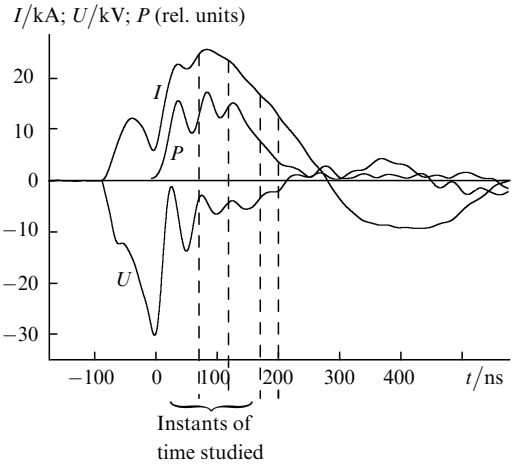

Figure 4. Oscillograms of the discharge current pulses I, voltage U across the peaking capacitor, and ASE P for $p = 4$ atm, Ne : Xe : HCl = 1400 : 10 : 1 and $U_0 = 30$ kV.

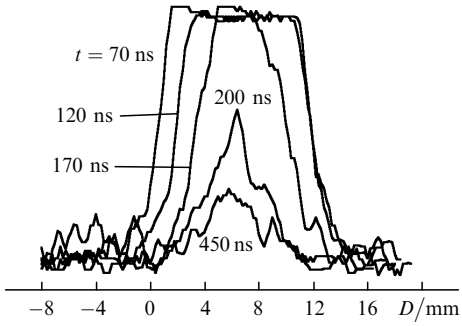

Figure 5. Densitogram of the disharge emission at different instants of time.

amplifying region decreases beginning from the moment $t = 100$ ns, whereas at the moment $t = 200$ ns the amplification occurs only in two narrow regions.

According to Figs. 5 and 6, we can separate several stages of the discharge burning. At the first stage, before the moment $t = 80 - 100$ ns, a homogeneous discharge is observed with the average current density of ~ 350 A cm^{-2}. At the next stage, the discharge is contracted in the region of the high electric field strength. This region corresponds to regions *2* and *3* in Fig. 7, in which the average current density increases to $700 - 800$ A cm^{-2}. In this case, macroinhomogeneities in the form of many channels with the transverse size of no more than $1 - 2$ mm appear from anode and cathode plasma spots in region 2. The channels are aligned in a row over the discharge-gap length with the linear density $n = 6 - 8$ cm^{-1} (at 120 ns), and burning in them occurs simultaneously with the volume discharge in region *3*.

By the moment $t = 170$ ns, a zone appears in region *3* on the anode side, where the propagating beam is not amplified (Fig. 7a). This region propagates towards the cathode, and after $25 - 30$ ns the volume discharge transforms to the filamentary discharge over entire region *3*. The filamentary structure can be observed upon detection of radiation using a more sensitive photographic film (Fig. 8). In this case, no plasma spots were observed on the anode.

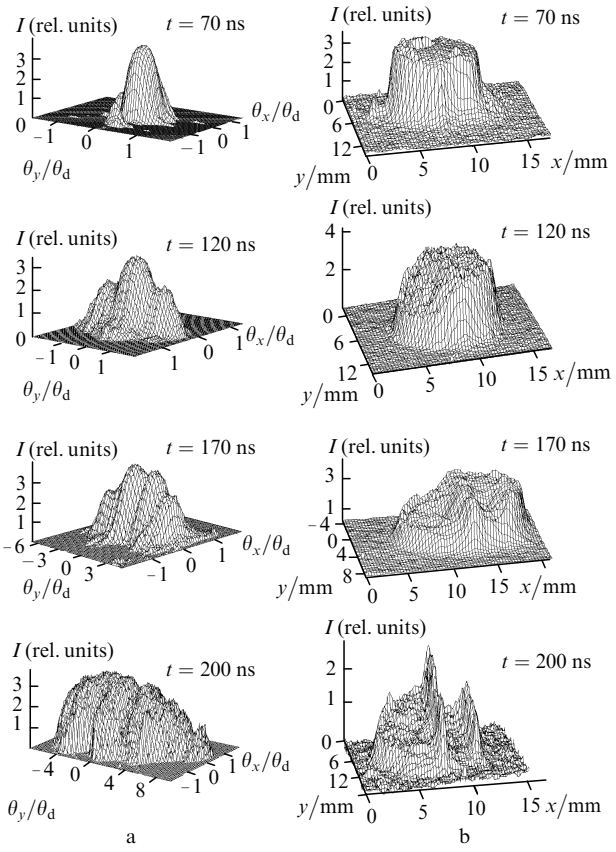

Figure 6. Distribution of the radiation intensity in the far-field (a) and near-field (b) zones at different instants of time; θ_d is the diffraction angle (for the homogeneous intensity distribution over the beam cross section).

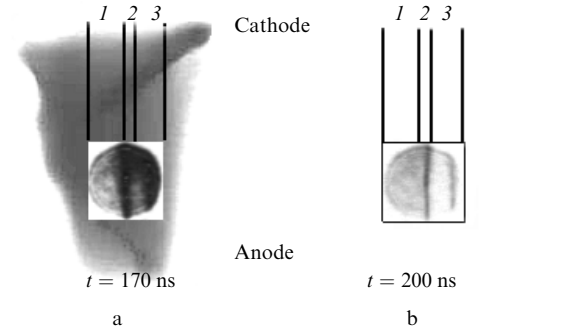

Figure 7. Time-integrated emission of the discharge gap (a) and the intensity distribution of the amplified beam related to the amplification region at different instants of time.

By the instant of time $t = 200$ ns, the properties of the active medium in region *3* change – it transforms from an amplifying medium to the absorbing one ($g_0/\alpha < 1$), with the absorption coefficient equal to 0.01 cm^{-1} at 308 nm (Fig. 7b). This property of the medium is retained up to the end of the first current period. This can be explained by the rapid burn-out of halogen in the filamentary channel because of the high density of the current in the channel [15, 16]. As a result, the gain in the filamentary channel drastically decreases, while the absorption coefficient remains the same [7]. At the same time in region *2* containing many macrochannels aligned over the discharge gap length, the input signal is still amplified by the time $t = 200$ ns, while the ratio g_0/α exceeds unity during the entire time of the discharge burning.

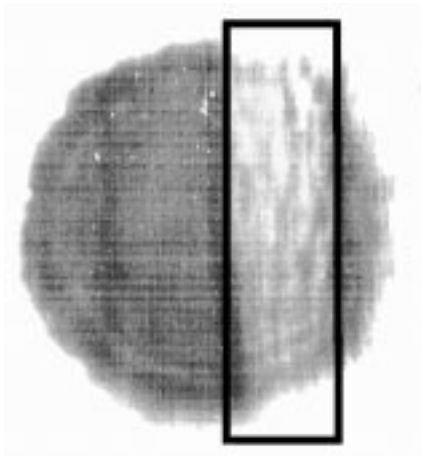

Figure 8. Distribution of the radiation intensity after the transit in the amplifier at the instant of time 200 ns.

Nevertheless, when the number of macrochannels in the discharge is small ($n < 1$ cm^{-1}, the inhomogeneous burning of the plasma sheet), the current flowing through the discharge gap is contracted into these channels, and the amplification in this region disappears much faster than in other regions. When the discharge leaves region *1*, the medium in this region does not noticeably affect the intensity and divergence of the laser beam propagating in it until the end of the first current period.

The deterioration of the divergence of the amplified radiation observed after the moment of time $t = 80$ ns can be explained both by the amplitude and phase inhomogeneity. The phase incursion on macroinhomogeneities will mainly occur due to the different electron density in the plasma and it can be estimated from the expression [26]

$$\left(\frac{\partial\varphi}{\partial z}\right)_e = -\frac{\pi n_e}{\lambda n_{cr}},$$

where $n_{cr} = 1.17 \times 10^{22}$ cm^{-3} is the critical electron density. Because in our case the macrochannels have a periodic structure along electrodes, the phase incursion on the length 60 mm is $\Delta\varphi = \pi/2$ for the difference of electron densities in the volume discharge and the channel $\Delta n_e \sim 10^{15}$ cm^{-3}. The estimate of the phase incursion in microchannels of size 200 μm with $n_e = 10^{17}$ cm^{-3} [15, 17] gives $\Delta\varphi = 0.8\pi$. In our opinion, the change in the refractive index should be mainly caused by thermal and shock waves, which appear upon gas-dynamic expansion of microchannels [14, 27]. In our case, this will be observed after the instant of time $t =$ 300 ns.

The deterioration of the angular divergence of the amplified beam caused by amplitude distortions is explained by a drastic change in the gain in the active medium over the laser beam cross section due to the redistribution of the current. We can separate two main moments of time in the change in the discharge width: $t = 120$ and 200 ns (Fig. 4). At the first stage, the divergence of the amplified radiation did not change, whereas at the second stage, it increased approximately by a factor of two. At the third stage, when the transverse size of the active medium was of about 1 mm, the beam divergence increased approximately by a factor of ten.

Fig. 9 shows the divergences of the amplified beam observed at different moments of the discharge burning in phase conjugation experiments. This figure presents the

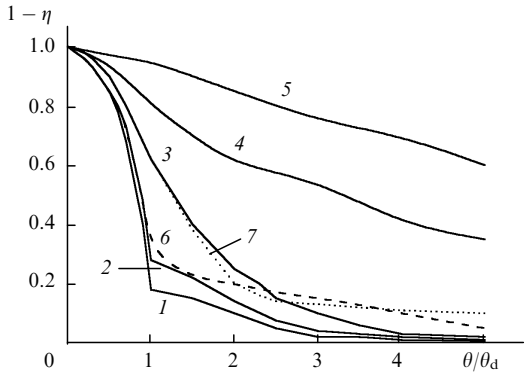

Figure 9. Angular directivity diagrams for the input (*1*), amplified (*2–5*), and conjugated (*6*, *7*) beams at instants of time $t = 70$ (*2*, *6*), 120 (*3*, *7*), 170 (*4*), and 200 ns (*5*); η is a fraction of the total radiation energy within the corresponding angle θ.

angular directivity diagrams for the amplified beam, the beam reflected from the SBS medium, and the beam amplified during the back transit. One can see from Fig. 9 that the directivity diagrams of the reflected beams obtained at the instants of time 70 and 120 ns are similar to those of the incident beams at the corresponding instants of time. In this case, the reflected beam contained $\sim 70\,\%$ of the pump-beam energy. A part of this energy (20 %) corresponded to the non-conjugated component, which had a broad directivity diagram. It seems likely that this component appeared due to the SBS noise.

At $t = 170 - 200$ ns, the amplitude distortions considerably increased (Fig. 5), and the reflected signal that repeatedly passed through the amplifier did not reconstruct the wave front of the initial beam.

4. Conclusions

Our study of the effect of various optical inhomogeneities on the divergence of the amplified radiation in the active medium of an electric-discharge XeCl laser excited by 300-ns pulses showed that, at the pump power density between 100 and 200 kW cm^{-3}, the radiation can be amplified with the diffraction-limited divergence, virtually without distortions in the active medium of the laser. At the pump power density between 400 and 500 kW cm^{-3}, optical macro- and microinhomogeneities appear in the discharge after the instant of time $t = 120$ ns, which impair the radiation divergence.

The radiation divergence is mainly determined by the redistribution of the gain profile in the active medium. In our case, the appearance of macroinhomogeneities results in the amplification, whereas the development of microinhomogeneities leads to absorption of some regions of the laser beam. The total influence of inhomogeneities existing in the laser medium results in the increase in the radiation diver-gence approximately by a factor of ten.

Up to the moment $t = 170$ ns after the discharge initiation, the use of phase conjugation allows one to retain the diffraction-limited divergence of the amplified beam. However, this methods becomes inefficient at later times.

Acknowledgements. The authors thank N G Ivanov for the discussion and help during the preparation of this paper.

References

1. Losev V F, Ivanov N G, Panchenko Yu N *Izv.Vyshch. Uchebn. Zaved., Ser. Fiz.* **42** 54 (1999)
2. Ivanov N G, Losev V F, Panchenko Yu N, Yastremsky A G *Kvantovaya Elektron.* **29** 14 (1999) [*Quantum Electron.* **29** 852 (1999)]
3. Zel'dovich B Ya, Pilipetskii N F, Shkunov V V *Obrashchenie volnovogo fronta* (Phase Conjugation) (Moscow: Nauka, 1985)
4. Ragul'skii V V *Obrashchenie volnovogo fronta pri vynuzhdennom rasseyanii sveta* (Phase Conjugation upon Stimulated Light Scattering) (Moscow: Nauka, 1990)
5. Korolev Yu D, Mesyatz G A *Fizika impul'snogo proboya gazov* (Physics of Pulsed Gas Breakdown) (Moscow: Nauka, 1991)
6. Taylor R S *Appl. Phys. B* **41** 1 (1986)
7. Taylor R S, Corkum P B, Watanabe S, Leopold K E, Alcock A J *IEEE J. Quantum Electron.* **19** 416 (1983)
8. Osborne M R, Hutchinson M H R *J. Appl. Phys.* **59** 711 (1986)
9. Dreiskemper R, Botticher W *IEEE Trans. Plasma Sci.* **23** 987 (1995)
10. Bychkov Yu, Makarov M, Suslov A, Yastremsky A *Rev. Sci. Instr.* **65** 28 (1994)
11. Baranov V Yu, Borisov V M, Stepanov Yu Yu *Elektrorazryadnye ksimernye lazery na galogenidakh inertnykh gazov* (Electric-Discharge Excimer Lasers on Halides of Inert Gases) (Moscow: Energoatomizdat, 1988)
12. Efimovskii S V, Zhigalkin A K, Karev Yu I, et al. *Preprint FIAN* No 79 (Troitsk, 1991)
13. Grasyuk A Z, Efimovskii S V, Zhigalkin A K, et al. *Preprint FIAN* No 18 (Moscow, 1989)
14. Borovkov V V, Andramanov A V, Voronov S L *Kvantovaya Elektron.* **26** 19 (1999) [*Quantum Electron.* **29** 19 (1999)]
15. Kushner M J *IEEE Trans. Plasma Sci.* **19** 387 (1991)
16. Dem'yanov A V, Kochetov I V, Napartovich A P, Kapitelli M, Longo S *Kvantovaya Elektron.* **22** 673 (1995) [*Quantum Electron.* **25** 645 (1995)]
17. Napartovich A P, Dem'yanov A V, Deryugin A A, Dyatko N A, Kochetov I V *Proc. SPIE Int. Soc. Opt. Eng.* **1625** 221 (1992)
18. Bahr M, Botticher W, Choroba S *IEEE Trans. Plasma Sci.* **19** 369 (1991)
19. Gower M C, Caro R G *Opt. Lett.* **7** 162 (1982)
20. Armandillo E, Prock D *Opt. Lett.* **8** 523 (1983)
21. Davis G M, Gower M C *IEEE J. Quantum Electron.* **27** 496 (1991)
22. Karpov V B, Korobkin V V, Dolgolenko D A *Kvantovaya Elektron.* **18** 1350 (1991) [*Sov J. Quantum Electron.* **21** 1235 (1991)]
23. Bychkov Yu I, Losev V F, Panchenko Yu N *Kvantovaya Elektron.* **19** 688 (1992) [*Sov. J. Quantum Electron.* **22** 638 (1992)]
24. Losev V F, Panchenko Yu N *Kvantovaya Elektron.* **24** 812 (1997)
25. Ragul'skii V V, Faizullov F S *Opt. Spektrosk.* **27** 707 (1969)
26. Dem'aynov A V, Deryugin A A, Dyatko N A *Kvantovaya Elektron.* **17** 1150 (1990) [*Sov J. Quantum Electron.* **20** 1060 (1990)]
27. Bychkov Yu I, Suslov A I, Tinchurin K A, Yastremsky A G *Preprint of Tomsk Scientific Centre, Siberian Division, Acad. of Sciences of USSR* No. 37 (Tomsk, 1990)